ARTICLE IN PRESS

Nuclear Instruments and Methods in Physics Research A ∎ (∎∎∎∎) ∎∎∎–∎∎∎

Contents lists available at ScienceDirect

Nuclear Instruments and Methods in Physics Research A

journal homepage: www.elsevier.com/locate/nima

The MAPS-based vertex detector for the STAR experiment: Lessons learned and performance

Giacomo Contin

Lawrence Berkeley National Laboratory, Berkeley, CA 94720, USA

for the STAR collaboration

ARTICLE INFO

Article history:
Received 4 December 2015
Received in revised form
21 April 2016
Accepted 30 April 2016

Keywords:
Pixel
MAPS
Heavy ions
Silicon tracker
STAR experiment
HFT

ABSTRACT

The PiXeL detector (PXL) of the STAR experiment at RHIC is the first application of the state-of-the-art thin Monolithic Active Pixel Sensors (MAPS) technology in a collider environment. The PXL, together with the Intermediate Silicon Tracker (IST) and the Silicon Strip Detector (SSD), form the Heavy Flavor Tracker (HFT), which has been designed to improve the vertex resolution and extend the STAR measurement capabilities in the heavy flavor domain, providing a clean probe for studying the Quark–Gluon Plasma.

The two PXL layers are placed at a radius of 2.8 and 8 cm from the beam line, respectively, and is based on ultra-thin high resolution MAPS sensors. The sensor features 20.7 μm pixel pitch, 185.6 μs readout time and 170 mW/cm^2 power dissipation. The detector is air-cooled, allowing a global material budget of 0.4% radiation length on the innermost layer. A novel mechanical approach to detector insertion allows for fast installation and integration of the pixel sub detector. The HFT took data in Au+Au collisions at 200 GeV during the 2014 RHIC run. Modified during the RHIC shutdown to improve its reliability, material budget, and tracking capabilities, the HFT took data in $p+p$ and $p+$Au collisions at $\sqrt{s_{NN}}=200$ GeV in the 2015 RHIC run.

In this paper we present detector specifications, experience from the construction and operations, and lessons learned. We also show preliminary results from 2014 Au+Au data analyses, demonstrating the capabilities of charm reconstruction with the HFT.

Published by Elsevier B.V.

1. Introduction

The PiXeL detector (PXL) of the STAR Experiment at the relativistic Heavy Ion Collider (RHIC), Brookhaven National Laboratory (BNL), is the first vertex detector based on the state-of-the-art MAPS technology to be operated in a collider environment. The PXL detector, together with the Intermediate Silicon Tracker (IST) and the Silicon Strip Detector (SSD), is part of the Heavy Flavor Tracker (HFT), which has been designed to extend the measurement capabilities of the STAR Experiment in the heavy flavor domain [1,2]. Heavy quark measurements are a key component for the systematic characterization of the dense medium created in heavy ion collisions, the so-called Quark–Gluon Plasma (QGP), which is one of the main goals of the STAR Experiment heavy ion program.

The STAR experiment uses a Time Projection Chamber (TPC) inside a 0.5 T magnetic field as its main tracking detector. With its 1 mm pointing resolution at the vertex, the TPC is not able to distinguish the decay vertices of short-lived heavy flavor particles, like D^0 mesons ($c\tau\sim120$ μm), in the high multiplicity environment typically produced in Au+Au collisions at $\sqrt{s_{NN}}=200$ GeV. The HFT, consisting of 4 cylindrical silicon detector layers, has been inserted inside the TPC inner field cage in 2014 to improve the track pointing resolution of the STAR detector (see Fig. 1). The outermost layer of the HFT is placed at 22 cm from the beam line and is equipped with the SSD: it is based on double sided silicon strip sensors with 95 μm inter-strip pitch and 35 mrad relative P-N-side stereo angle; the SSD silicon and front-end chips were part of an existing detector [3] and have been equipped with new faster electronics, allowing for a data acquisition rate up to 1 kHz. The IST is placed at 14 cm radius and based on single-sided silicon pad sensors with 600 μm × 6 mm pitch. The two innermost PXL layers are placed at 8 and 2.8 cm radius. In order to achieve the required track pointing resolution, STAR tracks inward with graded resolution from the TPC (resolution ~1 mm) to the vertex, by using the SSD and the IST intermediate resolution (~250–300 μm) to guide the tracks to the two innermost layers of PXL (~30 μm).

E-mail address: gcontin@lbl.gov

http://dx.doi.org/10.1016/j.nima.2016.04.109
0168-9002/Published by Elsevier B.V.

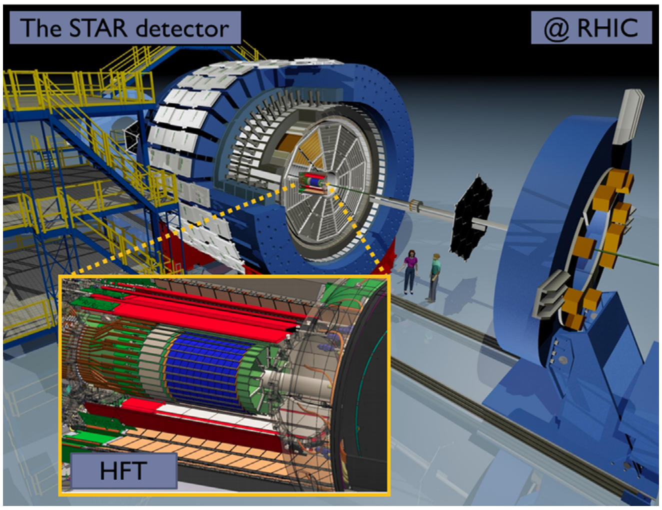

Fig. 1. Structure of the STAR HFT. The HFT consists of a three detector upgrade inserted in the TPC inner field cage.

The PXL detector design specifications, construction and expected performance are described in the following section of the paper. Section 3 describes the operational issues experienced during the first two years of data taking. The measured performance of the PXL detector and its contribution to the physics measurement of STAR are reported in Section 4.

2. The MAPS-based PXL detector

2.1. The ultimate-2 sensor

The PXL detector uses *Ultimate-2*, a sensor based on CMOS Monolithic Active Pixel Sensor (MAPS) technology, developed by IPHC in Strasbourg, France and optimized for the STAR experiment [4,5]. These sensors, thinned down to 50 μm to reduce their contribution to the material budget, use pixels with a pitch of 20.7 μm arranged in a 928 (rows) by 960 (columns) array (almost 1 Megapixel per sensor) on a $(20.22 \times 22.71)\,mm^2$ chip with a high-resistivity epitaxial layer to increase the radiation hardness and improve the signal-to-noise performance. The total signal for a MIP has been measured to be $\sim 1000\ e^-$, with a signal-to-noise ratio of about 30 for the pixel collecting most of the charge in the cluster. Each pixel includes readout and correlated double sampling (CDS) circuitry for signal extraction and noise subtraction. The reticle is divided into 4 sub-arrays to allow the process variation compensation with independent configurations of the reference voltages. The pixel array is read out by addressing one row at a time and processing all columns in parallel through programmable threshold discriminators located at the end of each column. The integration time of the whole sensor is 185.6 μs. The resulting digital data are then passed through a zero-suppression logic block located at the periphery of the pixel array on the same chip, which delivers encoded hit addresses for up to a maximum of 9 hit clusters per row; the data are then passed to on-chip memory intermediate buffering. The memory is arranged in two banks of 1500 words each allowing simultaneous read and write operations. The data are read out bit- serially from one of these memory banks over two Low-Voltage Differential Signaling (LVDS) outputs per sensor, each running at 160 MHz. Most of the sensor internal parameters can be programmed with a serial interface using the JTAG protocol. A low power dissipation of $170\ mW/cm^2$ allows these sensors to be operated at room temperature with just air cooling, resulting in a further reduction of the material budget.

Fig. 2. PXL half-detector: 5 sectors mounted in dovetail slots on the carbon fiber support and connected to the insertion mechanics.

The relatively short integration time (185.6 μs) and the radiation tolerance (up to 0.9 kGy/year and 2×10^{11} to 10^{12} 1 MeV n_{eq}/cm^2) meet the specifications imposed by the STAR experimental conditions.

2.2. The PXL construction

The PXL detector has been designed as a highly parallel system [6]. It is subdivided into 2 detector-halves attached on one side to a unique cantilevered support mechanics, allowing for fast insertion and retraction of the detector by manually sliding the detector-halves along rails inside a support cylinder and locking them into a reproducible position using kinematic mounts. Each half consists of 5 sectors mounted in dovetail slots. A sector represents the basic unit in terms of powering and readout and consists of a trapezoidal thin (250 μm) carbon fiber sector tube with four 10-sensor ladders mounted on each tube, one at the inner radius, and 3 at the outer radius, arranged in a turbo geometry design (see Fig. 2).

After being pre-diced through deep-reactive-ion-etching (DRIE) technique, thinned by grinding and diced, the sensors, fully probe tested and characterized, are positioned with butted edges on flex cables using acrylic adhesive and precision vacuum chucks [7]. The sensors and the first electronics board responsible for power distribution and signal buffering are electrically connected via standard wire bonding to the flex cable and the wires are encapsulated for protection. The structure is stiffened by a carbon fiber backer glued at the bottom of the flex cable. At this point, precision vacuum chucks are used to attach the ladders to the sector tubes. The ladder and sector assembly fixtures rely on a series of pins and holes for the alignment of the different components. Fully assembled sectors are surveyed in a coordinate measurement machine (CMM) with an accuracy of about 5 μm: the position of fiducial markers on the silicon sensors and the ladder surface profile are mapped and related to a set of 3 tooling balls mounted on the sectors. In this way a full map of the pixel positions on each sector is achieved. The completed sectors are then assembled into detector halves which are surveyed to form completely mapped stable units with the pixel positions known to an accuracy of approximately 10 μm. The ladder functionalities are tested after each assembly and position measurement step. Finally, the detector halves are attached to the insertion mechanics completing the detector assembly in preparation for installation into the STAR detector. In case of severe damage to the running detector, a novel approach to insertion mechanics allows replacing it with a spare detector copy within one day without interrupting beam operations [8].

2.3. The HFT track pointing resolution

The excellent pointing resolution of the HFT is driven by the unprecedented characteristics of the PXL, that with a small inner

Please cite this article as: G. Contin, Nuclear Instruments & Methods in Physics Research A (2016), http://dx.doi.org/10.1016/j.nima.2016.04.109

Download English Version:

https://daneshyari.com/en/article/8168526

Download Persian Version:

https://daneshyari.com/article/8168526

Daneshyari.com